Journal of Information Systems Engineering and Management
2025, 10(42s)
e-ISSN: 2468-4376
https://www.jisem-journal.com/

Research Article

Influence of Viscosity Changes on Magneto-Hydrodynamic Squeeze Film Lubrication Between Rough Circular Plates Using Couple-Stress Fluid

Latha Y. L.[1*] and Hanumagowda B. N.[1]
[1]*Department of Mathematics, School of Applied Sciences, REVA University, Bengaluru-560064, Karnataka, India*
Corresponding Author Email: lathamanju2214@gmail.com

ARTICLE INFO

Received: 30 Dec 2024
Revised: 12 Feb 2025
Accepted: 26 Feb 2025

ABSTRACT

This paper examines the influence of viscosity fluctuations and magnetic fields on squeeze film lubrication between rough circular plates using a couple-stress fluid. A modified Reynolds equation is derived based on Christensen's stochastic theory to account for surface roughness. The analysis specifically investigates two types of one-dimensional roughness patterns: radial and azimuthal. Expressions for pressure, load-carrying capacity, and squeeze film time are formulated, with discussions centred on the variation of various non-dimensional parameters, supported by 2D and 3D graphical representations. The results reveal that radial roughness tends to reduce, while azimuthal roughness increases, the pressure, load-carrying capacity, and squeeze film time. Furthermore, the presence of viscosity variation, couple stress, and magnetic fields significantly enhances these parameters compared to the smooth plate scenario. The study also calculates the relative percentage changes for these attributes, offering valuable insights for design engineers to optimize bearing performance by selecting appropriate surface structures, magnetic fields, and lubricant additives to prolong bearing life.

Keywords: Squeeze film, Viscosity variation, Roughness, MHD, Couple stress, Circular plates.

INTRODUCTION

Squeeze film behaviour plays a crucial role in a wide range of engineering and scientific fields, such as lubricated joints, gears, viscous dampers, bearings, as well as in the functioning of automotive and aircraft engines. A squeeze film refers to a thin layer of thick, sticky lubricant that forms between two surfaces when they approach each other. As the surfaces get closer, the viscous lubricant accumulates, resisting immediate squeezing out due to its thick nature. This resistance generates pressure within the lubricant film, which in turn supports the load. The application of squeeze films is critical in reducing wear and tear, providing damping, and ensuring smooth operation in mechanical systems. In classical hydrodynamic lubrication, studies by Pinkus [1], Cameron [2], and Hamrock [3] have largely assumed that lubricants behave as Newtonian fluids. However, recent experimental findings indicate that adding a small amount of high molecular weight polymers to a Newtonian fluid can yield more effective lubricants. This enhancement is particularly beneficial in applications where load-carrying capacity and response time are crucial, such as in bearing systems or automotive engines. To explain the behaviour of such non-Newtonian lubricants, micro-continuum theories, such as those developed by Ariman and Sylvester [4, 5] and Stokes [6], have been proposed. The Stokes micro-continuum theory extends classical fluid continuum theory by incorporating polar features like body couples and couple stresses. This theory has been applied in several studies [7-12] to investigate the impact of couple stresses on fluid-film bearings. The results suggest that using fluids with couple stresses lead to improved squeeze film performance, characterized by higher film pressure, increased load-carrying capacity, and longer response times. These findings have practical applications in optimizing the design of bearings, dampers, and other mechanical systems, where the use of couple-stress fluids can enhance performance, durability, and reliability in demanding engineering environments.

Journal of Information Systems Engineering and Management
2025, 10(42s)
e-ISSN: 2468-4376
https://www.jisem-journal.com/

Research Article

In recent years, Magnetohydrodynamics (MHD) has become an area of considerable interest in lubrication theory. Studies have demonstrated that the use of electrically conductive fluids can enhance the load-carrying capacity of bearings. Several theoretical investigations have indicated that electromagnetic fields have a beneficial effect on squeeze films, especially in applications involving high-speed operations and high external temperatures.

Couple stress fluid is commonly used as a lubricant in hydromagnetic bearings, offering several advantages over traditional solid bearings. Various studies have explored the MHD performance of bearings lubricated with electrically conductive fluids under the influence of a magnetic field, including research on smooth surfaces such as Kuzma's study on parallel plate slider bearings [13], Lin's work on annular disks [14], and Lin et al.'s investigation of curved annular plates [15]. These studies show that, compared to non-magnetic scenarios, the presence of a magnetic field leads to improvements in film pressure, load capacity, and squeeze film duration. It is important to note that most bearing surfaces exhibit some degree of roughness. All bearing surfaces typically exhibit some level of roughness, which plays a significant role in the field of tribology—the study of friction, lubrication, and wear between interacting surfaces. The mean separation of sliding surfaces and the height of roughness asperities in bearings are often of a similar magnitude. To better understand how surface roughness affects the performance of hydrodynamic bearings, various approaches have been proposed. The stochastic model introduced by Christensen [16] has been widely used as a foundation for studies on the hydrodynamic lubrication of rough surfaces. Many researchers have explored the combined effects of couple stress, MHD, and surface roughness. For instance, Bujurke et al. [17-18] studied rectangular and finite rectangular plates, Hanumagowda et al. [19-21] focused on curved circular, curved annular, and conical plates, and Salma et al. [22] investigated curved annular plates. These studies found that surface roughness enhances squeeze film performance, especially in cases of azimuthal roughness as opposed to radial patterns. However, viscosity variations are common in real-world scenarios and can significantly impact the lubrication process of bearings. Bartz and Ehlert [23] explored the effects of pressure-viscosity oils on the temperature, pressure, and film thickness in elasto-hydrodynamic rolling contacts. Hanumagowda [24] studied the squeeze film behavior of circular step bearings with varying viscosity in couplestress fluids, while Lin et al. [25] focused on parallel circular plates with viscosity considerations. Additionally, several researchers [26-30] have investigated the combined effects of roughness, pressure-viscosity dependence, and couplestress fluids on different bearing types. Most recently, Syeda et al. [31] examined the impact of MHD and surface roughness on the behavior of non-Newtonian squeeze films in circular plates. The primary goal of the present research is to analyze how viscosity variations influence the lubrication of squeeze films between circular plates, with a focus on the effects of surface roughness.

Mathematical Analysis

Figure 1 depicts the squeeze film lubrication between two circular plates, where the upper plate moves downward towards the lower rough plate at a velocity V . A magnetic field, represented by, is applied vertically along the z-axis. The film thickness between the plates is denoted by $'h'$, and 'a' represents radius of the circular plates.

The equation that governs the analysis of squeeze film characteristics is as follows:

$$\mu\frac{\partial^2 u}{\partial z^2}-\eta\frac{\partial^4 u}{\partial z^4}-\sigma B^2 u=\frac{\partial p}{\partial r} \qquad (1) \qquad \frac{\partial p}{\partial z}=0$$

(2)

$$\frac{\partial w}{\partial z}+\frac{1}{r}\frac{\partial(ru)}{\partial r}=0 \qquad (3)$$

Where σ is the conductivity of the lubricant, $'u'$and $'w'$ are the velocity component along r and $z-$directions respectively

Journal of Information Systems Engineering and Management
2025, 10(42s)
e-ISSN: 2468-4376
https://www.jisem-journal.com/

Research Article

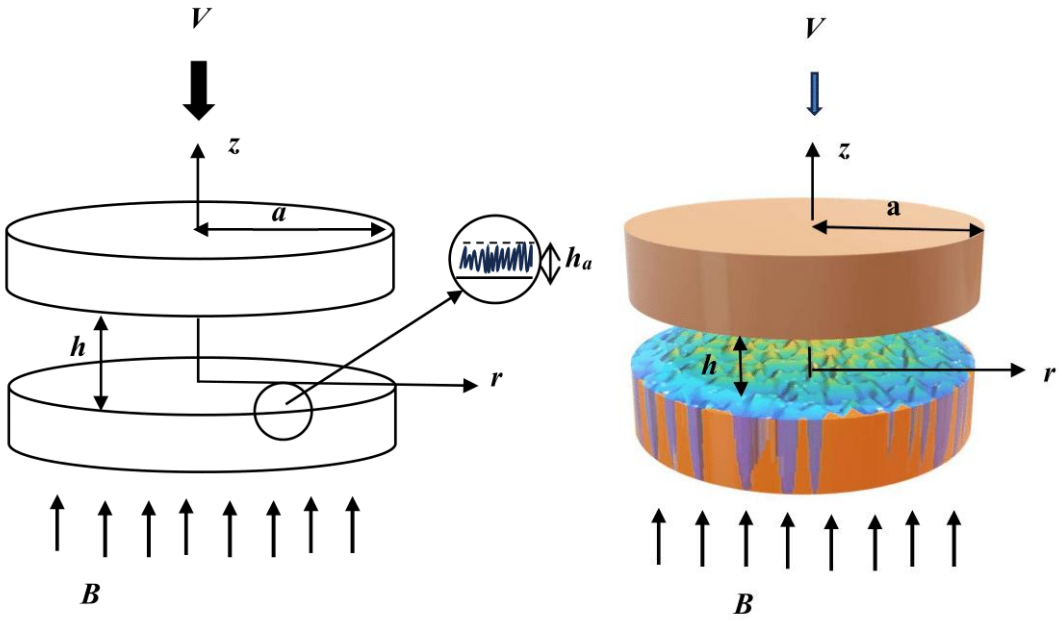

Figure 1: Geometry of rough circular plate

The following are required boundary conditions:

At $(z = h)$:

$$u = 0, \quad \frac{\partial}{\partial z}\left(\frac{\partial u}{\partial z}\right) = 0 \tag{4a}$$

$$w = -V. \tag{4b}$$

At $(z = 0)$:

$$u = 0 \quad , \quad \frac{\partial}{\partial z}\left(\frac{\partial u}{\partial z}\right) = 0 \tag{5a}$$

$$w = 0. \tag{5b}$$

Using boundary conditions (4a) and (5a) to solve equation (1), we obtain

$$u = \left\{\left(\chi_1 - \chi_2\right) - 1\right\} \frac{h_0^2}{\mu M^2} \frac{\partial p}{\partial x} \tag{6}$$

where, couple stress parameter is $k = \sqrt{\eta / \mu}$ and Hartmann number is $M = B h_0 \sqrt{(\sigma/\mu)}$.

$$\chi_1 = \chi_{11}, \ \chi_2 = \chi_{12} \qquad \text{for} \quad 4M^2k^2 / h_0^2 < 1 \tag{7a}$$

$$\chi_1 = \chi_{21}, \ \chi_2 = \chi_{22} \qquad \text{for} \quad 4M^2k^2 / h_0^2 = 1 \tag{7b}$$

$$\chi_1 = \chi_{31}, \ \chi_2 = \chi_{32} \qquad \text{for} \quad 4M^2k^2 / h_0^2 > 1 \tag{7c}$$

Journal of Information Systems Engineering and Management
2025, 10(42s)
e-ISSN: 2468-4376
https://www.jisem-journal.com/

Research Article

$$\chi_{11}=\frac{\alpha^2}{(\alpha^2-\beta^2)}\frac{\cosh\{\beta(2z-h)/2k\}}{\cosh(\beta h/2k)} \qquad \chi_{12}=\frac{\alpha^2}{(\alpha^2-\beta^2)}\frac{\cosh\{\alpha(2z-h)/2k\}}{\cosh(\alpha h/2k)}$$

$$\alpha=\sqrt{\frac{1+\sqrt{\left(1-4M^2k^2/h_0^2\right)}}{2}} \qquad \beta=\sqrt{\frac{1-\sqrt{\left(1-4M^2k^2/h_0^2\right)}}{2}}$$

$$\chi_{21}=\frac{2\cosh\left\{(z-h)/\sqrt{2}k\right\}+2\cosh\left(z/\sqrt{2}k\right)}{2\left\{\cosh\left(h/\sqrt{2}k\right)+1\right\}}$$

$$\chi_{22}=\frac{\left(z/\sqrt{2}k\right)\sinh\left\{(z-h)/\sqrt{2}k\right\}+\left\{(z-h)/\sqrt{2}k\right\}\sinh\left(z/\sqrt{2}k\right)}{2\left\{\cosh\left(h/\sqrt{2}k\right)+1\right\}}$$

$$\chi_{31}=\frac{\cos(\beta_2 z)\cosh\{\alpha_2(z-h)\}+\cosh(\alpha_2 z)\cos\{\beta_2(z-h)\}}{\cosh(\alpha_2 h)+\cos(\beta_2 h)}$$

$$\chi_{32}=\frac{\cot\theta\left\langle\sinh(\alpha_2 z)\sin\{\beta_2(z-h)\}+\sin(\beta_2 z)\sinh\{\alpha_2(z-h)\}\right\rangle}{\cosh(\alpha_2 h)+\cos(\beta_2 h)}$$

$$\theta=\tan^{-1}\left(\sqrt{\frac{4k^2M^2}{h_0^2}-1}\right),\ \alpha_2=\sqrt{\frac{M}{kh_0}}Cos\left(\frac{\theta}{2}\right),\ \beta_2=\sqrt{\frac{M}{kh_0}}Sin\left(\frac{\theta}{2}\right)$$

The substitute (6) in (3) and integrate over the thickness of the film and using the boundary conditions (4b) and (5b), we obtain

$$\frac{1}{r}\frac{\partial}{\partial r}\left\{\xi(h,k,M)\,r\frac{\partial p}{\partial r}\right\}=-\mu V \tag{8}$$

where, $\xi(h,k,M)=\begin{cases}\dfrac{h_0^2}{M^2}\left\{\dfrac{2k}{(\alpha^2-\beta^2)}\left(\dfrac{\beta^2}{\alpha}\tan h\dfrac{\alpha h}{2k}-\dfrac{\alpha^2}{\beta}\tan h\dfrac{\beta h}{2k}\right)+h\right\}, & \text{for } 4M^2k^2/h_0^2<1\\ \dfrac{h_0^2}{M^2}\left\{\dfrac{h}{2}\sec h^2\left(\dfrac{h}{2\sqrt{2k}}\right)-3\sqrt{2k}\tan h\left(\dfrac{h}{2\sqrt{2k}}\right)+h\right\}, & \text{for } 4M^2k^2/h_0^2=1\\ \dfrac{h_0^2}{M^2}\left\{\dfrac{2kh_0}{M}\left(\dfrac{(\alpha_2\cot\theta-\beta_2)\sin\beta_2 h-(\beta_2\cot\theta+\alpha_2)\sin\alpha_2 h}{\cos\beta_2 h+\cosh\alpha_2 h}\right)+h\right\}, & \text{for } 4M^2k^2/h_0^2>1\end{cases}$

The fluid film thickness is expressed through a mathematical formula divided into two components, one accounting for the smooth surface and the other for the influence of surface roughness.

$$H=h+h_a(r,\theta,\xi). \tag{9}$$

Let $g(h_a)$ denote the probability distribution function of the stochastic film thickness h_a. Taking the expected value of equation (8) with respect to $g(h_a)$ results in the modified Reynolds equation.

Journal of Information Systems Engineering and Management
2025, 10(42s)
e-ISSN: 2468-4376
https://www.jisem-journal.com/

Research Article

$$\frac{1}{r\mu}\frac{\partial}{\partial r}\left\{r\frac{\partial E(p)}{\partial r}\times E\{\xi(H,k,M)\}\right\}=-V \qquad (10)$$

where, $E\ (*)=\int_{-\infty}^{\infty}(*)\,g\,(h_a)\,d\,h_a$

According to Christensen [7] we assumed that $g\,(h_a)=\begin{cases}\frac{35}{32\,c^7}(c^2-h_a^2)^3, & -c<\ h_a<\ c\\ 0 & \text{otherwise}\end{cases}$

where, standard deviation is $\bar{\sigma}$ and $\bar{\sigma}=c/3$

A one-dimensional rough surface consists of two distinct components: radial and azimuthal roughness patterns.

Radial roughness refers to surface variations that extend outward from the centre of the plate, following the radial direction. These roughness features are arranged in patterns that radiate from the centre to the edge of the plate.

The film thickness is $H=h+h_a(\theta,\xi)$ (11)

The Reynolds equation (10) is expressed as:

$$\frac{\partial}{\partial r}\left\{E\{\xi(H,k,M)\}r\frac{\partial E(p)}{\partial r}\right\}=-r\mu V \qquad (12)$$

Azimuthal roughness describes surface irregularities that follow concentric circles around the centre of the plate, oriented in the angular or circumferential direction. The roughness features are aligned in a circular pattern around the centre, parallel to the plate's circumference.

The film thickness is: $H=h+h_a(r,\ \xi)$ (13)

The stochastic Reynolds equation (10) is expressed as:

$$\frac{\partial}{\partial r}\left\{\frac{1}{E\left(\frac{1}{\xi\ (H,\ k,M)}\right)}r\ \frac{\partial E(p)}{\partial r}\right\}=-r\mu V \qquad (14)$$

Let us combined equation (12) and (14) into a single expression as follows.

$$\frac{1}{r}\frac{\partial}{\partial r}\left\{\Phi(H,\ k,M,\ C)\ r\frac{\partial E(p)}{\partial r}\right\}=-\mu V\ , \qquad (15)$$

where,

$$\Phi(H,k,M,C)=\begin{cases}E(\xi(H,k,M)) & \text{for radial roughness}\\ [E(1/\xi(H,k,M))]^{-1} & \text{for azimuthal roughness}\end{cases}$$

$$E(\xi(H,k,M))=\frac{35}{32\,c^7}\int_{-c}^{c}\xi(H,k,M)(c^2-h_a^2)^3\,d\,h_a\ ,$$

Journal of Information Systems Engineering and Management
2025, 10(42s)
e-ISSN: 2468-4376
https://www.jisem-journal.com/

Research Article

$$E\left(\frac{1}{\xi(H,k,M)}\right)=\frac{35}{32c^7}\int_{-c}^{c}\frac{(c^2-h_a^2)^3}{\xi(H,k,M)}\,d\,h_a\,.$$

Viscosity-pressure dependency relation is given by the authors Barus [32] and Bartz and Ether [23] as

$$\mu=\mu_0 e^{\beta p} \tag{16}$$

where, μ_0 represent viscosity at constant temperature and ambient pressure and β is pressure-dependent viscosity co-efficient.

Following dimensionless parameters are defined:

$$k^*=\frac{2k}{h_0},\ r^*=\frac{r}{a}\ ,\ h^*=\frac{h}{h_0},C=\frac{c}{h_0},\ p^*=\frac{ph_0^3}{\mu_0 a^2(-dh/dt)}\quad ,\ \nu=\frac{\beta\mu_0 a^2(-dh/dt)}{h_0^3}$$

Introducing the above dimensional parameter in equation (15), it becomes

$$\frac{1}{r^*}\frac{\partial}{\partial r^*}\left\{e^{-\nu p^*}\Phi^*(H^*,k^*,M,C)r^*\frac{\partial P^*}{\partial r^*}\right\}=-1 \tag{17}$$

where,

$$\Phi^*(H^*,k^*,M,C)=\begin{cases}E(\xi^*(H^*,k^*,M)), & \text{for radial roughness}\\ \{E(1/(\xi^*(H^*,k^*,M)))\}^{-1}, & \text{for azimuthal roughness}\end{cases}$$

$$E(\xi^*(H^*,k^*,M))=\frac{35}{32c^7}\int_{-c}^{c}\xi^*(H^*,k^*,M)(c^2-h_a^2)^3\,d\,h_a$$

$$E\left(\frac{1}{\xi^*(H^*,k^*,M)}\right)=\frac{35}{32c^7}\int_{-c}^{c}\frac{(c^2-h_a^2)^3}{\xi^*(H^*,k^*,M)}\,d\,h_a$$

$$\xi^*(H^*,k^*,M)=\begin{cases}\frac{1}{M^2}\left\{\frac{l^*}{(\alpha^{*2}-\beta^{*2})}\left(\frac{\beta^{*2}}{\alpha^*}\tanh\frac{\alpha^*H^*}{k^*}-\frac{\alpha^{*2}}{\beta^*}\tanh\frac{\beta^*H^*}{k^*}\right)+H^*\right\} & \text{for}\quad M^2k^{*2}<1\\ \frac{1}{M^2}\left\{\frac{H^*}{2}Sech^2\left(\frac{H^*}{\sqrt{2}\,k^*}\right)-\frac{3k^*}{\sqrt{2}}\tanh\left(\frac{H^*}{\sqrt{2}\,k^*}\right)+H^*\right\} & \text{for}\quad M^2k^{*2}=1\\ \frac{1}{M^2}\left\{\frac{k^*\left(\alpha_2^*Cot\,\theta^*-\beta_2^*\right)Sin\,\beta_2^*H^*-k^*\left(\beta_2^*Cot\,\theta^*+\alpha_2^*\right)Sinh\,\alpha_2^*H^*}{M\left(Cos\,\beta_2^*H^*+Cosh\,\alpha_2^*H^*\right)}+H^*\right\} & \text{for}\quad M^2k^{*2}>1\end{cases}$$

$$\alpha^*=\left\{\frac{1+(1-M^2k^{*2})^{1/2}}{2}\right\}^{1/2}\qquad \beta^*=\left\{\frac{1-(1-M^2k^{*2})^{1/2}}{2}\right\}^{1/2}$$

$$\theta^*=\tan^{-1}\left(\sqrt{k^{*2}M^2-1}\right),\ \alpha_2^*=\sqrt{\frac{2M}{k^*}}Cos\left(\frac{\theta^*}{2}\right),\ \beta_2^*=\sqrt{\frac{2M}{k^*}}Sin\left(\frac{\theta^*}{2}\right)$$

The boundary conditions for the non-dimensional pressure are as follows.

Journal of Information Systems Engineering and Management
2025, 10(42s)
e-ISSN: 2468-4376
https://www.jisem-journal.com/

Research Article

$$\frac{d P^*}{d r^*} = 0 \quad \text{at} \quad r^* = 0, \quad \text{and} \quad P = 0 \quad \text{at} \quad r^* = 1 \tag{18}$$

By integrating the non-dimensional Reynolds equation (17) with respect to r^* and applying the boundary conditions, we can express the non-dimensional film pressure as.

$$P^* = -\frac{1}{\nu}\ln\left\{1-\frac{\nu\,(1-r^{*2})}{4\Phi^*(H^*,k^*,M,C)}\right\} \tag{19}$$

The expressions for the load-supporting capacity is

$$W = 2\pi\int_0^a p\,r dr$$

The load-supporting capacity is obtained in the following form

$$W^* = \frac{W h_0^3}{\mu_0 a^3 (d h/d t)} = -\frac{1}{\nu}\int_0^1\left[\ln\left\{1-\frac{\nu(1-r^{*2})}{4\Phi^*(H^*,k^*,M,C)}\right\}\right]dr^* \tag{20}$$

The nondimensional response time T^* is introduced by:

$$T^* = \frac{t h_0^2}{\mu_0 a^3} = -\frac{1}{\nu}\int_{h_1^*}^1\int_0^1 \ln\left\{1-\frac{\nu(1-r^{*2})}{4\Phi^*(H^*,k^*,M,C)}\right\} d r^*\, d h^* \tag{21}$$

where, $h_1^* = \dfrac{h_1}{h_0}$

RESULT AND DISCUSSION

This study explores the impact of viscosity variation, MHD effects, couple stress fluids, and surface roughness on squeeze film lubrication between circular plates. The analysis focuses on several non-dimensional parameters, including the viscosity variation parameter, Hartmann number, couple stress parameter, and roughness parameter. These factors are essential for understanding the behaviour of the lubricant film under various conditions. To evaluate their influence on critical performance aspects such as pressure distribution, load-carrying capacity, and squeeze film duration, specific ranges of these parameters are considered in the study.

$\nu = 0, 0.002, 0.004, \quad M = 0, 2, 4, \quad k^* = 0, 0.2, 0.4, \quad C = 0, 0.2, 0.4$

Dimensionless Pressure

In Figure 2, the dimensionless pressure P^* is outlined against the radial coordinate r^* for varying values of C, showcasing both roughness patterns. The findings reveal a distinct trend: as C increases, the pressure rises for the azimuthal roughness pattern, while it experiences a decline for the radial roughness pattern, illustrating the contrasting effects of surface texture on lubrication performance. Fig 3 illustrates the graph of P^* as function of r^* for various of ν. For both roughness configurations, it is observed that P^* rises with rising ν values. Fig 4 and Fig 5 represents the various results of P^* versus r^* for different values of M and k^*.

Journal of Information Systems Engineering and Management
2025, 10(42s)
e-ISSN: 2468-4376
https://www.jisem-journal.com/

Research Article

Table 1: Comparison of present analysis with Syeda et al [31] with $k^* = 0.4, M = 2, \quad h^* = 0.8, r = 0.4$ and $h_1^* = 0.5$

		Syeda et al [31]		Present analysis			
				$\nu = 0$		$\nu = 0.004$	
	C	radial	azimuthal	radial	azimuthal	radial	azimuthal
	0	7.00517	9.33524	7.00541	9.33567	7.10518	9.51399
P^*	0.2	6.90492	9.90897	6.90516	9.90946	7.00207	10.11069
	0.4	6.62348	12.22769	6.62370	12.22843	6.71280	12.53684
	0	7.40893	7.40892	7.40926	7.40925	7.54412	7.54411
W^*	0.2	7.24941	7.86426	7.24972	7.86463	7.37877	8.01683
	0.4	6.81716	9.70451	6.81744	9.70508	6.93138	9.93836
	0	3.83122	3.83122	3.83164	3.83164	4.01620	4.01619
T^*	0.2	3.66041	4.28501	3.66078	4.28558	3.82111	4.54409
	0.4	3.26248	7.30202	3.26274	7.30464	3.37630	9.14623

Table 2: Variation of R_{P^*}, R_{W^*} and R_{T^*} for distinct values of C and ν with $k^* = 0.4, M = 2,$ $h^* = 0.8, r = 0.4$ and $h_1^* = 0.5$

		R_{P^*}		R_{W^*}		R_{T^*}	
C	ν	radial	azimuthal	radial	azimuthal	radial	azimuthal
	0.002	0.70359	0.94058	0.89604	0.89604	2.27917	2.27918
0	0.004	1.42418	1.91009	1.82015	1.82015	4.81646	4.81673
	0.006	2.15875	2.90487	2.76910	2.76910	7.66510	7.66538
	0.002	0.69339	0.99934	0.87644	0.95185	2.08370	2.81174
0.2	0.004	1.40344	2.03068	1.77992	1.93511	4.37994	6.03207
	0.006	2.12695	3.09128	2.70699	2.94647	6.92448	9.78628
	0.002	0.66488	1.23728	0.82362	1.17845	1.67343	8.69227
0.4	0.004	1.34516	2.52199	1.67129	2.40379	3.48019	25.21109
	0.006	2.03783	3.85250	2.53965	3.67250	5.43284	49.07490

It is observed that the pressure P^* reaches its maximum at $r^* = 0$, and further increases as the values of M and k^* rise. In all the figures 2-5, solid line represents the azimuthal and dash line radial pattern. The roughness properties of a surface are closely related to the pressure changes in fluid flow over that surface. An increase in surface roughness typically leads to greater variations in pressure because the surface imperfections restrict the fluid's smooth flow and cause pressure changes along the interface. Furthermore, compared to radial roughness, the pressure distribution

Journal of Information Systems Engineering and Management
2025, 10(42s)
e-ISSN: 2468-4376
https://www.jisem-journal.com/

Research Article

associated with azimuthal roughness is more apparent in all the figures 2-5. Furthermore, figure -6 represents three-dimensional graph of pressure distribution by varying surface parameter and viscosity, keeping $M = 2, k^* = 0.2, h_m^* = 0.5, r^* = 0.6$ constant as we noticed that pressure is significant due to increases in viscosity and effect is seen in for azimuthal than radial pattern. Also, variation of pressure with respect to M and k^* is depicted in figure-7 keeping $C = 0.3, \nu = 0.004$, $h_m^* = 0.5$, $r^* = 0.6$ constant. From figure it is observed that pressure is maximum at $M = 3$ & $k^* = 0.3$ as compared to $M = 0$ & $k^* = 0$. The introduction of a magnetic field leads to a significant accumulation of lubricant in the film regions, resulting in an increase in squeeze film pressure. This enhancement occurs due to the magnetic field's influence, which draws more lubricant into the film, amplifying the pressure generated during the squeeze process.

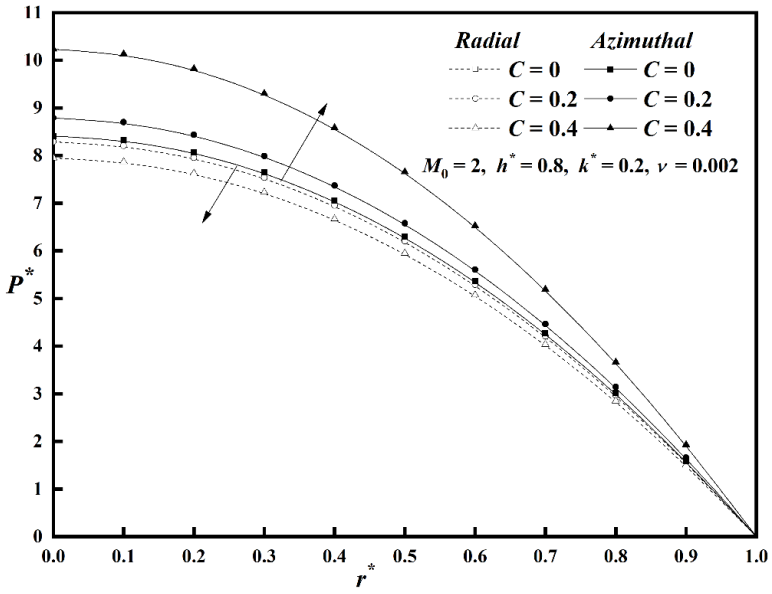

Figure 2: Graph of P^* versus r^* varying C values

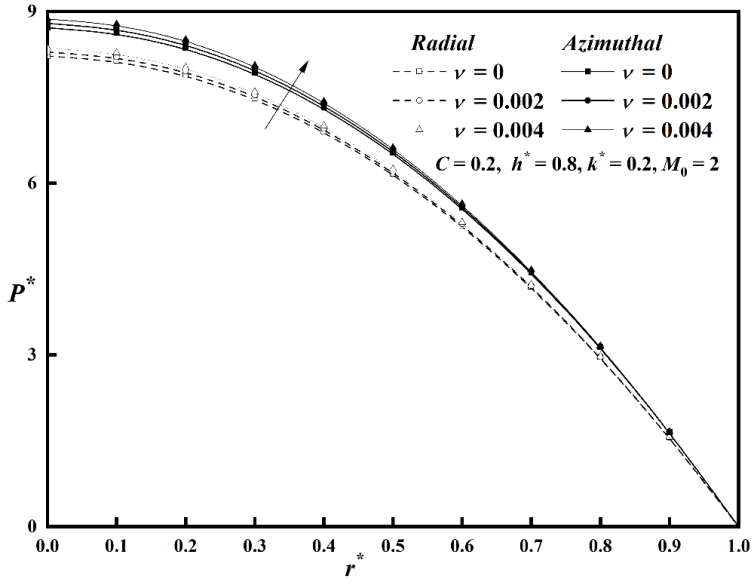

Figure 3: Plot of P^* versus r^* for distinct ν values

Journal of Information Systems Engineering and Management
2025, 10(42s)
e-ISSN: 2468-4376
https://www.jisem-journal.com/

Research Article

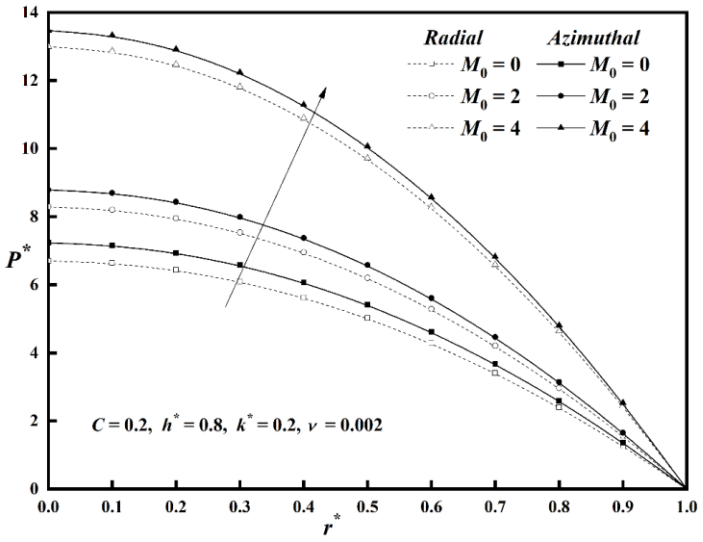

Figure 4: Graph of P^* versus r^* for distinct M values

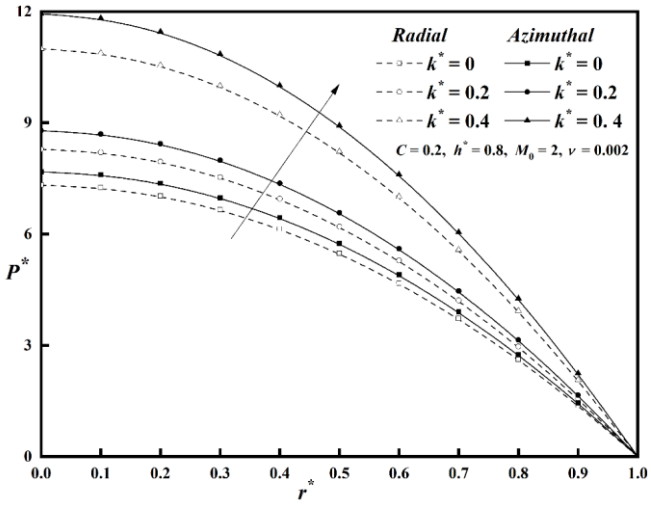

Figure 5: Graph of P^* versus r^* for different k^* values

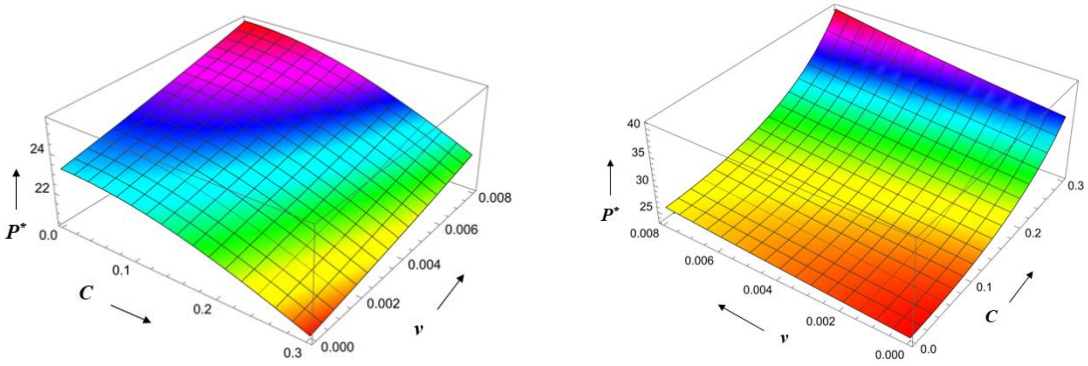

(a) Radial Roughness (b) Azimuthal Roughness

Figure 6: Graph of P^* Versus C and ν with $M = 2$, $k^* = 0.2$, $h_m^* = 0.5$, $r^* = 0.6$

Journal of Information Systems Engineering and Management
2025, 10(42s)
e-ISSN: 2468-4376
https://www.jisem-journal.com/

Research Article

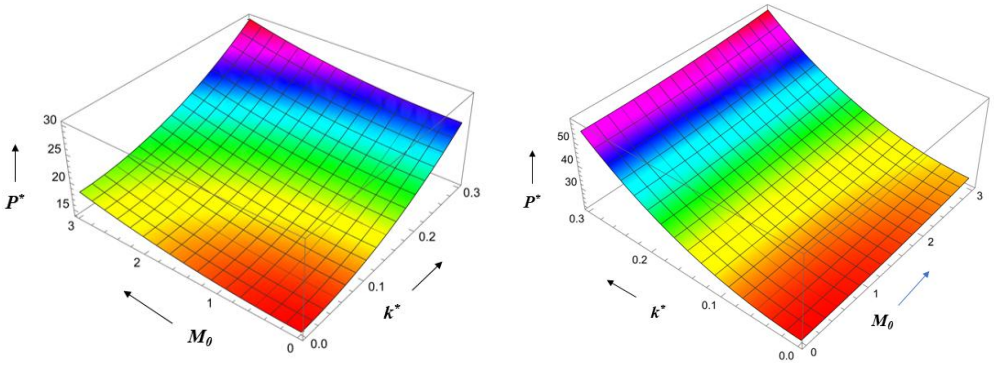

(a) Radial Roughness (b) Azimuthal Roughness

Figure 7: Graph of P^* Versus M and k^* with C = 0.3, ν = 0.004, h_m^* = 0.5, r^* = 0.6.

Load-supporting Capacity

Figure 8 depicts the plot of the non-dimensional load-supporting capacity W^* as a function of h^* for various values of C showcasing both rough surface patterns. As seen in the figure, both roughness configurations coincide at $C=0$, highlighting that at this value, the load-supporting capacity is the same for both surface types. Also, azimuthal roughness is found to have a more load-carrying capacity than radial roughness. The variation of W^* along with h^* for distinct values of ν is presented in Fig 9. The effect of viscosity variation observed to result in higher value of W^* Fig. 10 and Fig. 11 shows the variation of W^* against h^* for various values of M and k^* for both roughness surfaces and it is seen that W^* decreases for increasing values of h^*. Further, it is found that increasing values of M and k^* is to increases the load-supporting capacity. Additionally, figure -12 represents three-dimensional graph of load supporting capacity by varying surface parameter and viscosity, keeping $M = 2, k^* = 0.2, h_m^* = 0.5$ constant. It is observed that viscosity effect enhances the load for azimuthal pattern than radial. Also, variation of load with respect to M and k^* is presented in figure-13 keeping $C = 0.3, \nu = 0.004, h_m^* = 0.5$ constant. From the graph it is seen that load is maximum for increasing values of M & k^* as compared to $M=0$ & $k^*=0$. When a magnetic field is applied, a substantial quantity of lubricant accumulates in the film areas, increasing the squeezing film pressure which enhances the load supporting capacity.

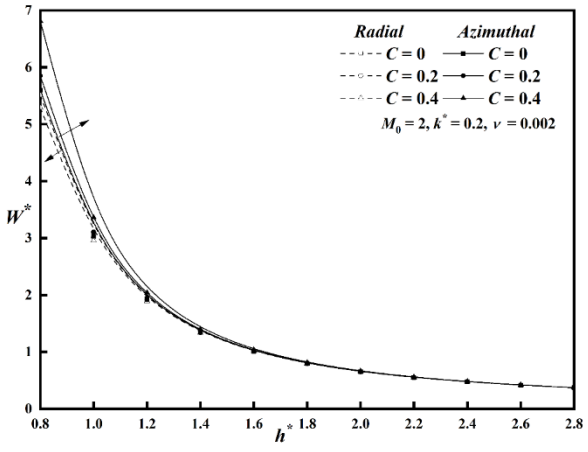

Figure 8: Graph of W^* versus h^* for various C values

Journal of Information Systems Engineering and Management
2025, 10(42s)
e-ISSN: 2468-4376
https://www.jisem-journal.com/

Research Article

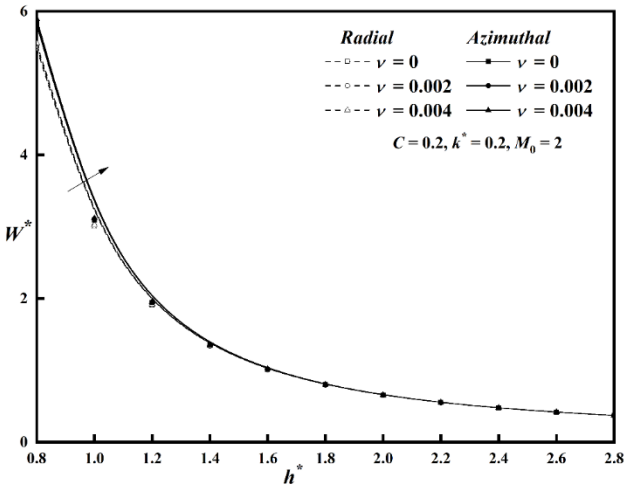

Figure 9: Graph of W^* versus h^* for distinct ν values

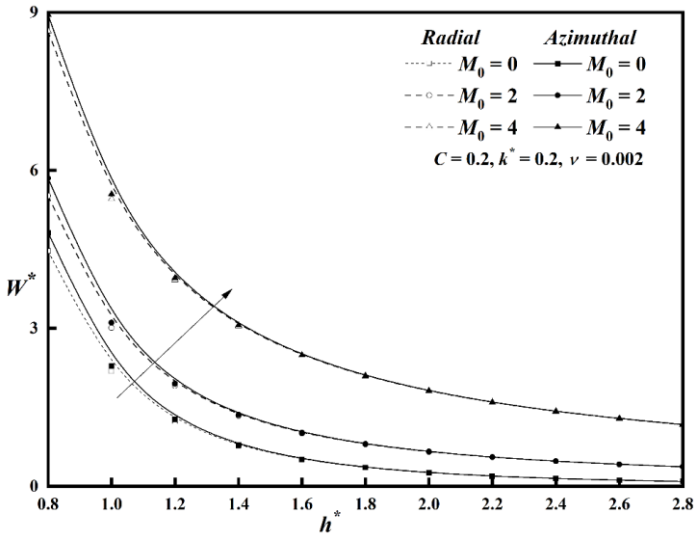

Figure 10: Graph of W^* versus h^* for different M values

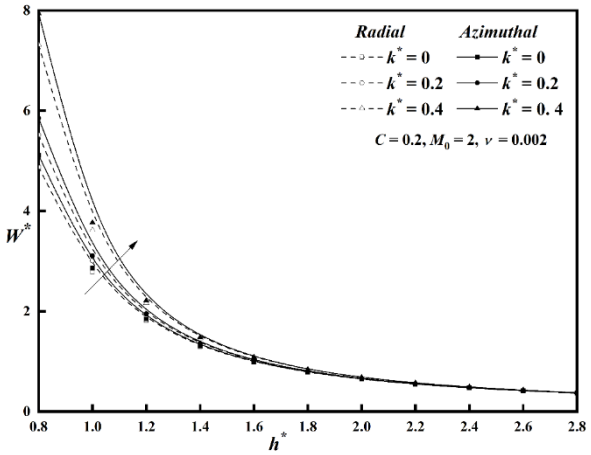

Figure 11: Graph of W^* versus h^* for different k^*

Journal of Information Systems Engineering and Management
2025, 10(42s)
e-ISSN: 2468-4376
https://www.jisem-journal.com/

Research Article

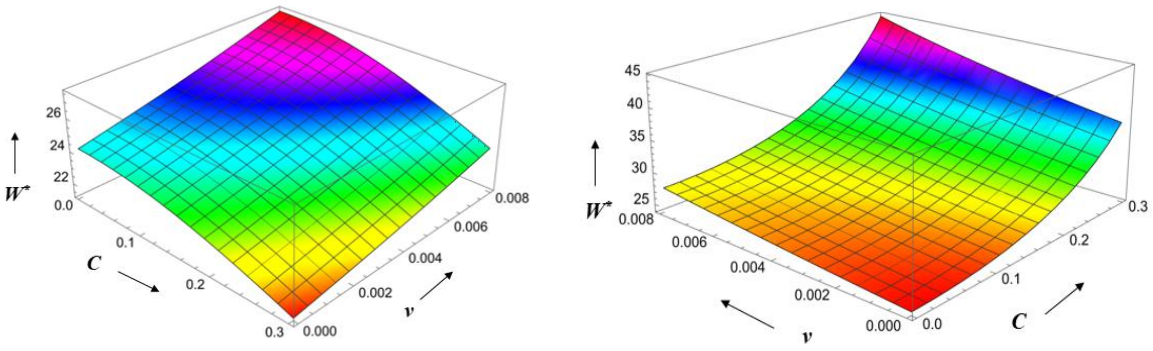

(a) Radial Roughness (b) Azimuthal Roughness

Figure 12: W^* Versus C and v with M = 2, k^* = 0.2, $h_m{}^*$ = 0.5.

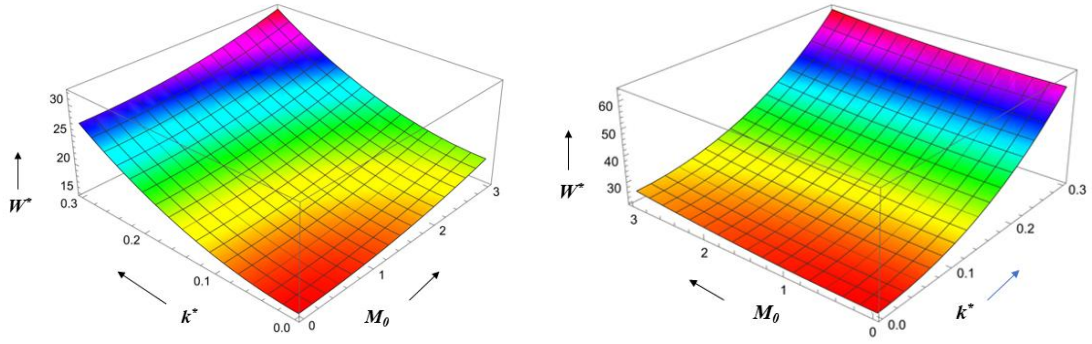

(a) Radial Roughness (b) Azimuthal Roughness

Figure 13: W^* Versus M and k^* with C = 0.3, v = 0.004, $h_m{}^*$ = 0.5.

Squeeze Film Time

Figure 14 shows the relationship between nondimensional squeeze film time T^* and h_1^* for different values of C . It is observed that as the value of C increases, the squeezing time significantly increases for azimuthal roughness, while it decreases for radial roughness. Furthermore, it is noted that both roughness patterns converge at $C=0$.

Fig. 15 depicts T^* variation with h_1^* for various values of ν for both the roughness configurations. As a result, increasing values of ν enhances the time T^* and it is shown that T^* declines for rise in h_1^* . Fig. 16 and Fig. 17 represents variation of T^* versus h_1^* for various M and k^* . A notable increase in T^* is observed with the rise in the magnetic field and couple stress parameter, as compared to the non-magnetic and Newtonian fluid cases. Fig18 presents the 3D graphs of squeeze film time for various values of viscosity parameter and surface roughness keeping $M = 2, k^* = 0.2, h_1^* = 0.5$ constant. Due to raise in roughness parameter and viscosity parameter, there is significant increase in squeeze film and more pronounced in case azimuthal than radial roughness. Further variation of squeeze film time with respect to magnetic field and couple stress parameter is depicted in figure 19 keeping $C = 0.3, \nu = 0.004, h_1^* = 0.5$ fixed. As a result, squeeze film time is maximum due increase in both parameters M & k^* when compared to $M = 0 \& k^* = 0$. As the Hartmann number and couple stress parameter increase, the squeeze film time is found to be longer for the azimuthal roughness pattern than for the radial roughness. This

Journal of Information Systems Engineering and Management
2025, 10(42s)
e-ISSN: 2468-4376
https://www.jisem-journal.com/

Research Article

indicates that the azimuthal configuration is more responsive to these factors, resulting in improved lubrication performance and extended film support times under the specified conditions.

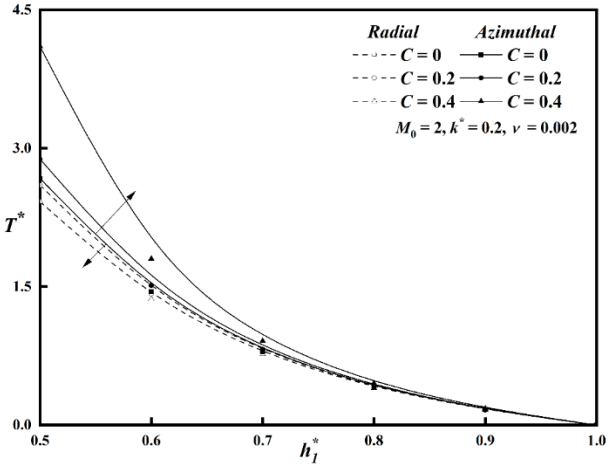

Figure 14: Graph of T^* versus h^*_1 for various C values

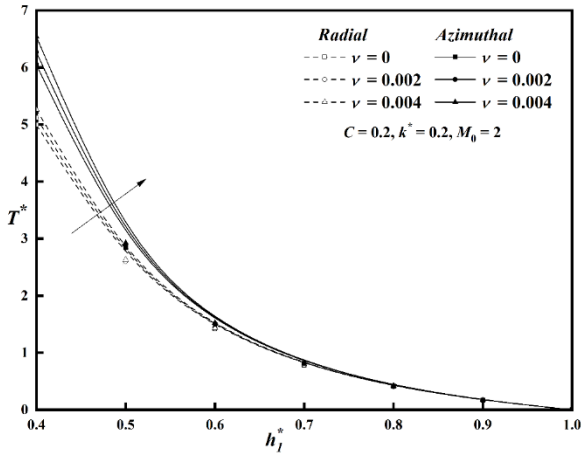

Figure 15: Graph of T^* versus h^*_1 for distinct ν values

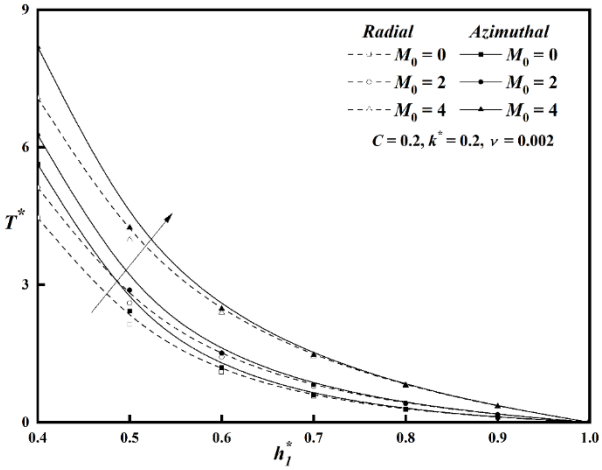

Figure 16: Graph of T^* versus h^*_1 for various M values

Journal of Information Systems Engineering and Management
2025, 10(42s)
e-ISSN: 2468-4376
https://www.jisem-journal.com/

Research Article

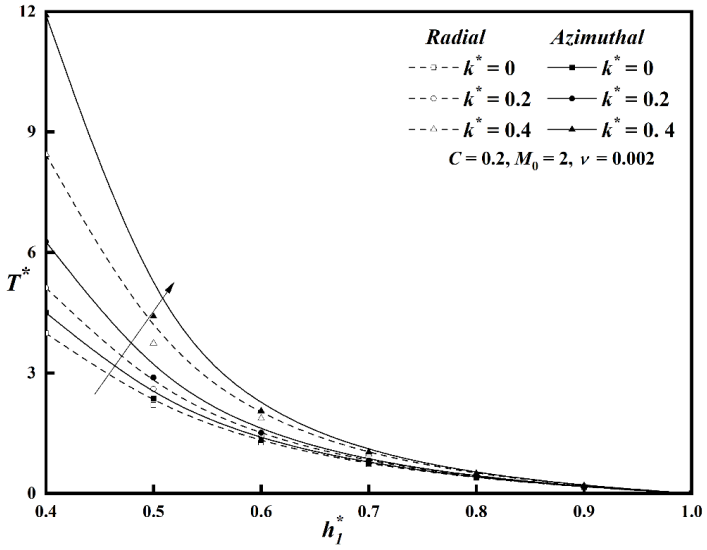

Figure 17: Graph of T^* versus h^*_1 for various k^* values

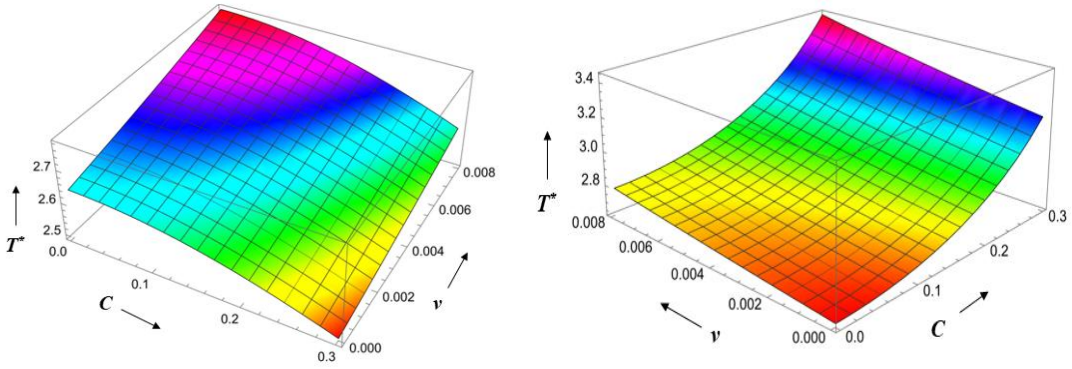

(a) Radial Roughness (b) Azimuthal Roughness

Figure 18: T^* Versus C and v with $M = 2$, $k^* = 0.2$, $h_1^* = 0.5$.

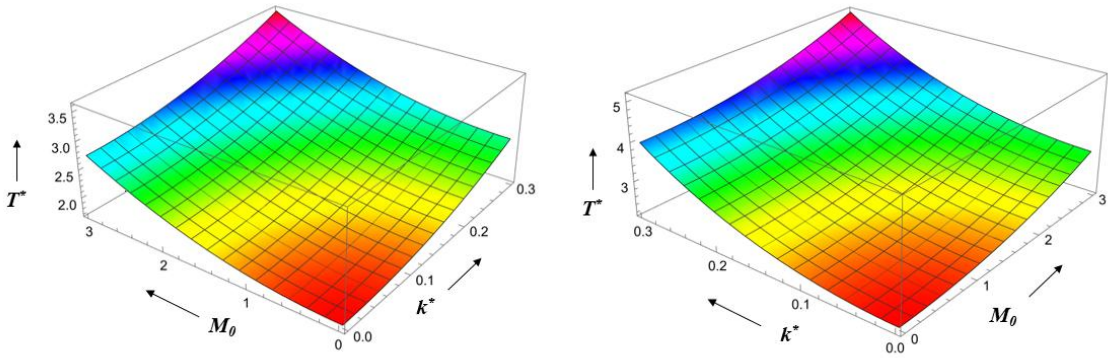

(a) Radial Roughness (b) Azimuthal Roughness

Figure 19: T^* Versus M and k^* with $C = 0.3$, $v = 0.004$, $h_1^* = 0.5$.

Journal of Information Systems Engineering and Management
2025, 10(42s)
e-ISSN: 2468-4376
https://www.jisem-journal.com/

Research Article

CONCLUSION

Based on the analysis of surface roughness, viscosity variation, and MHD effects on the lubrication of couple stress fluid between circular plates, the following conclusions can be made:

1. In comparison to smooth plates, the squeeze film pressure, load-carrying capacity, and squeeze film time of rough circular plates are either increased or decreased, depending on the roughness pattern. Specifically, the one-dimensional azimuthal roughness pattern enhances these parameters, while the radial roughness pattern has the opposite effect. This is because azimuthal roughness results in a larger contact area, which improves fluid retention and pressure buildup more effectively than the radial pattern.
2. Furthermore, the inclusion of lubricant additives and the presence of surface roughness are found to substantially enhance squeeze film performance when compared to Newtonian and non-magnetic cases. These factors collectively improve both the load-carrying capacity and squeeze film time, resulting in more efficient and long-lasting lubrication.
3. As $\nu \to 0$, the outcome for both one-dimensional circular plate roughness patterns can be reduced to a non-viscous case in the limiting scenario, as Syeda Tasneem Fathima et al. [31] investigated and shown in Table-1.
4. An increase in viscosity improves the performance of a squeeze film bearing by increasing the dimensionless pressure, enhancing the load-supporting capacity, and prolonging the response time. The increased viscosity makes the lubricant more resistant to flow, which helps to better support the load and respond more effectively under varying conditions.
5. The relative pressure, relative load and relative squeeze film time are calculated and tabulated in Table-2 with $k^* = 0.4, M = 2, h^* = 0.8, r = 0.4$ and $h_1^* = 0.5$. As result it is found that an increase of nearly 49% (5%), 4% (3%) and 4 % (%2) in T^*, W^* & P^* is observed for azimuthal (radial) roughness pattern

REFERENCES

[1] O. Pinkus and B. Sternlicht, Theory of Hydrodynamic Lubrication, McGrawHill, New York, NY, USA, 1961.
[2] A. Cameron, The Principles of Lubrication, Longmans, Green and Company, London, UK, 1966.
[3] B. J. Hamrock, Fundamentals of Fluid Film Lubrication, McGraw-Hill, New York, NY, USA, 1994.
[4] T. Ariman, M. A. Turk, and N. D. Sylvester, “Microcontinuum fluid mechanics-a review,” International Journal of Engineering Science, vol. 11, no. 8, pp. 905–930, 1973.
[5] T. Ariman, M. A. Turk, and N. D. Sylvester, “Applications of micro continuum fluid mechanics,” International Journal of Engineering Science, vol. 12, no. 4, pp. 273–293, 1974.
[6] V. K. Stokes, “Couple stresses in fluids,” Physics of Fluids, vol.9, pp. 1709–1715, 1966.
[7] G. Ramanaiah, Squeeze films between finite plates lubricated by fluids with couple stress. *Wear*. Vol. 54 (2): pp. 315-320, 1979. https://doi.org/10.1016/0043-1648(79)90123-6.
[8] N. M. Bujurke and G. Jayaraman, “The influence of couple stresses in squeeze films,” International Journal of Mechanical Sciences, vol. 24, no. 6, pp. 369–376, 1982.
[9] J. R. Lin, “Squeeze Film Characteristics of Finite Journal Bearings: Couple Stress Fluid Model”, *Tribology International*, vol. 31(4), pp. 201– 207, 1998.
[10] Jaw-Ren Lin., "Squeeze film characteristics between a sphere and a flat plate: couple stress fluid model," Computers & Structures, vol. 75, (1), pp. 73-80, 2000. https://doi.org/10.1016/S0045-7949(99)00080-2.
[11] N. B. Naduvinamani and A. Siddangouda, "Squeeze film lubrication between circular stepped plates of couple stress fluids," Braz Soc Mech Sci Eng, vol. 31 (1), pp. 21-26, 2009. https://doi.org/10.1590/S1678-58782009000100004.
[12] Biradar Kashinath., "Squeeze film lubrication between parallel stepped plates with couplestress fluids," International Journal of Statistika and Mathematika, vol. 3, (2), pp. 65-69, 2012.
[13] D. C. Kuzma, "The magnetohydrodynamic parallel plate slider bearing," ASME Journal of Basic Enginnering, vol. 87, (3), pp. 778-780, 1964. https://doi.org/10.1115/1.3650685.
[14] Jaw-Ren Lin., "Magneto-hydrodynamic squeeze film characteristics between annular disks," Industrial Lubrication and Tribology, vol. 53, (2), 66-71, 2001. https://doi.org/10.1108/00368790110384028.

[15] J. R. Lin, R. F. Lu and W. H. Liao, "Analysis of magnetohydrodynamic squeeze film characteristics between curved annular plates", Industrial Lubrication and Tribology, vol. vol. 56, (5), pp. 300-305, 2004. https://doi.org/10.1108/00368790410550714.

[16] H. Christensen, 'Stochastic models for hydrodynamic lubrication of rough surfaces', Proc Inst Mech Engg, vol. 184, pp. 1013-1022, 1969.

[17] N. M. Bujurke and R. B. Kudenatti, "MHD lubrication flow between rough rectangular plates," Fluid Dynamics Research, vol. 39, no. 4, pp. 334–345, 2007.

[18] N. M. Bujurke, N. B. Naduvinamani, and D. P. Basti, "Effect of surface roughness on magnetohydrodynamic squeeze film characteristics between finite rectangular plates," Tribology International, vol. 44, no. 7-8, pp. 916–921, 2011.

[19] B. N. Hanumagowda, A. Salma and C. S. Nagarajappa, "Effects of surface roughness, MHD and couple stress on squeeze film characteristics between curved circular plates", Journal of Physics: Conference Series, Vol.1000. Issue 1, 2018.

[20] B. N. Hanumagowda and A. Salma, "Combined effect of MHD, couple stress and surface roughness on curved annular plates", IJREAM, vol.4. Issue 6, pp-433-439, 2018.

[21] B. N. Hanumagowda, A. Salma and Swapna S Nair., "Combined effect of rough surface with MHD on porous conical bearing with conducting couple-stress fluid ", PJM, Vol. 10, Special Issue I, pp- 59-68, 2021.

[22] A. Salma and B. N. Hanumagowda, "Study of Surface Roughness with MHD and Couple Stress Fluid on Porous Curved Annular Plates" *Acta Polytechnica,* vol. 62, Issues 06, pp 574-588, 2022. https://doi.org/10.14311/AP.2022.62.0574.

[23] W. J. Bartz and J. Ether, Influence of pressure viscosity oils on pressure, temperature and film thickness in elastohydrodynamically lubricated rolling contacts, ProcI MechE, Part C: J Mechanical Engineering Science, vol. 222, pp. 1271–1280, 2008.

[24] B. N. Hanumagowda, Combined effect of pressure-dependent viscosity and couple stress on squeeze film lubrication between circular step plates, J of Eng tribology, vol. 229(6), pp. 1056-1064, 2015.

[25] J. R. Lin, L. M. Chu, L. J. Liang, Effects of viscosity dependency on the non-Newtonian squeeze film of parallel circular plates, Lub Sci,vol. 25, pp. 1–9, 2012.

[26] A. Siddangouda, T. V. Biradar, N. B. Naduvinamani, Combined effects of surface roughness and viscosity variation due to additives on long journal bearings, Tribology Materials, Surfaces and Interface, vol. 7(1), pp. 21-35, 2013.

[27] N. B. Naduvinamani, A. Siddangouda , A. G. Hiremath, Effect of surface roughness and viscosity pressure dependency on couple stress squeeze film lubrication of parallel circular plates, Advances in Tribology, vol. 2014, pp. 1-7, 2014.

[28] Noor Jahan, B. N. Hanumagowda, A. Salma and H. M. Shivakumar., Combined effect of piezo-viscous dependency and Couple Stresses on Squeeze-Film Characteristics of Rough Annular Plates, Journal of Physics: Conference Series, Vol.1000. Issue 1, 2018.

[29] Haewon Byeon, Y. L. Latha, B. N. Hanumagowda, Vediyappan Govindan, A. Salma, Sherzod Abdullaev, Jagadish V. Tawade, Fuad A. Awwad & Emad A. A. Ismail. "Magnetohydrodynamics and viscosity variation in couple stress squeeze film lubrication between rough flat and curved circular plates", Scientific Reports, Vol.13, Article number: 22960, 2023. https://www.nature.com/articles/s41598-023-50326-7.

[30] A. Salma, B. N. Hanumagowda, C. K. Sreekala, Taseer Muhammad, "Insight into the dynamics of couple-stress fluid through the porous medium between a curved circular plate and a rough flat plate: comparative analysis between radial and azimuthal roughness", Chinese Journal of Physics, vol. 88, pp. 991-1009, 2024.

[31] Syeda Tasneem Fathima. N. B. Naduvinamani., J. Santhosh Kumar., B. N. Hanumagowda, "Effect of surface roughness on the squeeze film characteristics of circular plates in the presence of conducting couple stress fluid and transverse magnetic field". *Advances in Tribology*, pp. 1–7, 2015.

[32] C. Barus. "Isothermals, isopiestics and isometrics relative to viscosity". *American Journal of Science*, vol. s3-45(266), pp. 87–96, 1893.